Near-Infrared Spectra of the Black Hole X-ray Binary A0620-00

Cynthia S. Froning[1]

cfroning@casa.colorado.edu

Center for Astrophysics and Space Astronomy, University of Colorado, 593 UCB, Boulder, CO 80309-0593

Edward L. Robinson

elr@astro.as.utexas.edu

Department of Astronomy, University of Texas at Austin, Austin, TX 78712

and

Martin A. Bitner

mbitner@astro.as.utexas.edu

Department of Astronomy, University of Texas at Austin, Austin, TX 78712

ABSTRACT

We present broadband NIR spectra of A0620-00 obtained with SpeX on the IRTF. The spectrum is characterized by a blue continuum on which are superimposed broad emission lines of H I and He II and a host of narrower absorption lines of neutral metals and molecules. Spectral type standard star spectra scaled to the dereddened spectrum of A0620-00 in K exceed the A0620-00 spectrum in J and H for all stars of spectral type K7V or earlier, demonstrating that the donor star, unless later than K7V, cannot be the sole NIR flux source in A0620-00. In addition, the atomic absorption lines in the K3V spectrum are too weak with respect to those of A0620-00 even at 100% donor star contribution, restricting the spectral type of the donor star in A0620-00 to later than K3V. Comparison of the A0620-00 spectrum to scaled K star spectra indicates that the CO absorption features are significantly weaker in A0620-00 than in field dwarf stars. Fits of scaled model spectra of a Roche lobe-filling donor star to the spectrum of A0620-00 show that the best match to the CO absorption lines is obtained when the C abundance is reduced to [C/H] = -1.5. The donor star contribution in the H waveband is determined to be $82 \pm 2\%$. Combined with previous published results from Froning & Robinson (2001) and Marsh et al. (1994), this gives a precise mass for the black hole in A0620-00 of $M_1 = 9.7 \pm 0.6$ $M_\odot$.

Subject headings: binaries: close — infrared: stars — stars: individual (A0620–00) — stars: variables: other

1. Introduction

Among X-ray binary systems (XRBs), 18 or more have been identified as containing probable black hole (BH) accretors (McClintock & Remillard 2005). The BH masses measured to date appear to fall into a limited range. From a Bayesian analysis of the observational parameters of several low-mass XRBs, Bailyn et al. (1998) concluded that 6 of the 7 systems measured had BH masses clustered around 7 $M_{\odot}$and that the overall population was heavily biased away from low BH masses (3 – 5 $M_{\odot}$). Since that study, at least one system, J0422+32, has been found to have a measured mass of about 4 $M_{\odot}$(Gelino & Harrison 2003), but the overall trend toward higher BH masses persists.

This result is in conflict with theoretical evolutionary models of the formation of BH XRBs, which predict a continuous distribution of BH masses from neutron star masses up to 10–15 $M_{\odot}$ (Fryer & Kalogera 2001). Confirmation or elimination of the low-mass BH "gap" would provide important constraints on the role of massive star evolution, supernova energetics, and subsequent binary evolution in BH formation (Fryer & Kalogera 2001). Further analysis of the mass distribution of BHs in compact binary systems is currently hampered by the generally poor precision of existing mass estimates (e.g., see Table 4.2 in McClintock & Remillard 2005). In this manuscript, we address this limitation by analyzing near-infrared (NIR) spectra to obtain a precise BH mass for one XRB, A0620-00.

A0620-00 was discovered in 1975 when it erupted in an X-ray nova (Elvis et al. 1975). After its return to quiescence, A0620-00 was revealed as an interacting binary system with a K star donating mass via an accretion disk to a compact object (Oke 1977; McClintock et al. 1983). Later, the orbital period of the binary and the radial velocity amplitude of the donor star were measured and yielded a mass function, $f(M) = 3.17\ M_{\odot}$, which established A0620-00 as a likely BH XRB (McClintock & Remillard 1986). Further observations established the binary mass ratio and determined the masses of the stars to within one unknown, the binary orbital inclination: $M_1 = (3.09 \pm 0.09) \sin^3 i\ M_{\odot}$ and $M_2 = (0.21 \pm 0.09) \sin^3 i\ M_{\odot}$, where M_1 and M_2 are the BH and donor star masses, respectively (Marsh, Robinson & Wood 1994;

[1]Visiting Astronomer at the Infrared Telescope Facility, which is operated by the University of Hawaii under Cooperative Agreement no. NCC 5-538 with the National Aeronautics and Space Administration, Science Mission Directorate, Planetary Astronomy Program.

Orosz et al. 1994). Several groups have determined values for the inclination, with the numbers ranging from $38^\circ \leq i \leq 75^\circ$. As a result, estimates of the BH mass in A0620-00 vary from 3.3 to 13.6 $M_\odot$(Haswell et al. 1993; Shahbaz, Naylor & Charles 1994; Froning & Robinson 2001; Gelino et al. 2001).

The broad range of derived inclinations and BH masses for A0620-00 result from long-term variability in the system and from uncertain determinations of the amount of veiling, or dilution, by sources other than the donor star. The inclination is determined by modeling the amplitude of the ellipsoidal variations in the donor star light curve, so both of these effects will alter the derived BH mass. In particular, an additional source will dilute the amplitude of the ellipsoidal variation, leading to an underestimate of the inclination and a corresponding overestimate of the BH mass if not taken into account.

The best way to determine the true donor star contribution in A0620-00 is to model its spectrum, particularly in the NIR, where the late type donor star is expected to dominate. Shahbaz, Bandyopadhyay & Charles (1999) modeled a low S/N, K-band spectrum of A0620-00, from which they concluded that the accretion disk contributes at most 27% of the continuum in the NIR. They fit only the ^{12}CO bandhead at 2.29 μm, however, which is sensitive to both temperature and luminosity of the donor star and may be prone to metallicity effects in compact binary systems (Froning & Robinson 2001). Harrison et al. (2007) also recently published a K-band spectrum of A0620-00 in which they confirmed that the ^{12}CO absorption lines are anomalously weak. What is needed to settle the debate over the contribution of the accretion disk to the NIR spectrum of A0620-00 are higher S/N, broadband spectra. To this end, we have obtained and present here 0.8 – 2.4 μm spectroscopy of A0620-00 obtained with SpeX at the NASA InfraRed Telescope Facility (IRTF). This manuscript is organized as follows: § 2 summarizes the data reduction and calibration steps; § 3 presents the data analysis and modeling of the donor star spectrum; and § 4 gives discussion and conclusions.

2. Observations and Data Reduction

We observed A0620-00 on 2004 January 8 – 10 using SpeX on the IRTF (Rayner et al. 2003). The weather was clear with good seeing conditions ($\lesssim 0.7''$) throughout the run. We observed A0620-00 using the ShortXD mode, which has a cross-dispersed echelle configuration and covers 0.8 – 2.5 μm simultaneously in 6 orders. All observations were obtained through the $0\farcs5$ slit, resulting in a spectral resolution in the center of each order of R = 1200 (250 km s^{-1}). A nearby A0V star was observed hourly to sample the atmospheric absorption spectrum. We also observed several spectral type calibration stars in the same configuration used for A0620-00 (supplemented with similar data from a previous SpeX observing run). The observations are summarized in Table 1.

All data reduction, calibration, and spectral extraction steps were performed using Spextool, an IDL-based package developed by the IRTF (Cushing, Vacca, & Rayner 2004; Vacca, Cushing, & Rayner 2003). The calibration processing steps included flat-fielding, sky subtraction, optimal spectral extraction, and wavelength calibration. Each A0620-00 exposure was extracted individually to preserve the full 300 sec time resolution. The spectra were corrected for telluric absorption and flux-calibrated using the A0V stellar spectra as described by Vacca, Cushing, & Rayner (2003). Finally, the orders were merged for each exposure to create single spectra covering the full wavelength range. The S/N per resolution element was ∼4 in the individual spectra. The slit was kept aligned to the parallactic angle during data acquisition, so the relative fluxes along the full $0.8 - 2.4$ μm range are accurate to $\leq 2\%$ (where the upper limit is the uncertainty at 0.9 μm when guiding at 2.4 μm; Cushing et al. 2004). In addition, stable observing conditions resulted in absolute flux calibrations of comparable quality. We have not quantified this number as our analysis does not depend on the absolute flux of the spectrum, but we note for completeness that a rough comparison of our mean in-band colors to those of Froning & Robinson (2001) and Gelino et al. (2001) yielded JHK colors within 0.1 mag of their results, well within the level of variability observed in A0620-00 over long time periods.

For the time-averaged spectrum of A0620-00, we shifted each 300 sec spectrum to the rest frame of the donor star before median combining, using the orbital ephemeris of McClintock & Remillard (1986) and the donor star radial velocity amplitude from Marsh, Robinson & Woo (1994). The error bars were determined by calculating the median absolute deviation of each pixel and then propagated through the smoothing and de-reddening steps. We did not correct for the effects of orbital smearing within an exposure time, but we note that this is a negligible effect ($\leq$30 km s^{-1}) at our 250 km s^{-1} spectral resolution. The time-averaged spectrum is shown in Figure 1. The spectrum has been boxcar-smoothed by 3 pixels, equivalent to one resolution element. Based on the scatter around linear fits to (relatively) line-free spectral regions, we find that the S/N in the time-averaged spectrum is ∼55 in H and K and ∼45 in J ($> 1\mu$m, ∼30 at shorter wavelengths).

Also shown in Figure 1 is the dereddened spectrum of A0620-00, calculated assuming a reddening along the line of sight of E(B–V) = 0.39 (Wu et al. 1976). Figures 2 – 4 show expanded views of the J,H, and K bands of the spectrum, with prominent spectral absorption and emission features labeled. Line identifications were made using multiple sources, including Wallace et al. (2000), Meyer et al. (1998), Kleinmann & Hall (1986), Harrison et al.

(2004), and the Atomic Line List[2].

3. Analysis

The broadband NIR spectrum of A0620-00 shown in Figures 1 – 4 is characterized by a blue continuum on which are superposed broad (full width at zero intensities $\geq$4000 km s^{-1}) emission lines of H I and He II and narrow (full width at half minima $\simeq$ 250 – 400 km s^{-1}) absorption lines of neutral metals, including transitions of Na I, Mg I, Al I, Si I, K I, Ca I, Ti I, and Fe I. The emission lines are believed to originate in the accretion disk, while the absorption features originate in the photosphere of the donor star. The absorption spectrum is similar to that of a K star, with previous estimates of the spectral type ranging from K3V to K7V (Oke 1977; González Hernández et al. 2004).

In Figure 5, we show the dereddened spectrum of A0620-00 compared to that of a field K5V star. The K star has been normalized to A0620-00 near 2.29 μm, just blueward of the ^{12}CO (2,0) bandhead. The comparison immediately shows that a K5V (or hotter) star cannot be the only flux source in the NIR. If the K5 star is scaled to the flux of A0620-00 in the K band, it exceeds the dereddened flux by >20% at bluer wavelengths. Adopting the K4V and K3V spectral types of Gelino et al. (2001) and González Hernández et al. (2004) results in an even larger disparity between the expected and observed J- and H-band fluxes. Even a spectral type as late at K7V exceeds the observed flux in A0620-00 by up to 10% over most of the J and H bands when normalized to 100% contribution in K.

Modest increases in the assumed reddening along the line of sight do not reconcile the spectrum of A0620-00 with that of a K5V star. Adopting a reddening of E(B–V) = 0.45 brings the 0.8 μm fluxes into agreement, but the template spectrum is still brighter than the spectrum of A0620-00 at longer wavelengths, including most of the J and H bands. Because the relative reddening values between H and K are small, the reddening must be increased to E(B–V) > 1.0 to bring the spectrum of the normalized K5V template below the spectrum of A0620-00 at all NIR wavelengths. It is extremely difficult to reconcile a reddening this high with the observed depth of the interstellar absorption feature at 2200 Å in the spectrum of A0620-00 (Wu et al. 1976). As a result, the fundamental conclusion remains: if the donor star is the sole source of NIR emission in A0620-00, its spectral type must be later than that of a K7V. Otherwise, some level of dilution must be present.

The absorption spectrum of A0620-00 resembles that of the K5V template, but there

[2]http://www.pa.uky.edu/p̃eter/atomic/

is at least one important difference between them: the CO molecular absorption features in A0620-00 are significantly weaker relative to the metal lines than in the template spectrum. This difference can affect determinations of the donor star contribution to the NIR spectrum. For example, the dilution analysis performed by Shahbaz, Bandyopadhyay & Charles (1999) on the K-band spectrum of A0620-00 is unlikely to be a valid determination of the contribution of the donor star to the NIR spectrum, since they relied entirely on the relative strength of the ^{12}CO 2.29 μm feature. The weakness of the CO lines also suggests that other anomalies may exist in the spectrum, necessitating that its decomposition be undertaken over a wide wavelength range and using multiple line species and features. Accordingly, we compare the line equivalent widths and line ratios in A0620-00 with those of field star populations and model the spectrum using both spectral type standards and synthetic spectra.

3.1. Classification Based on Spectral Indices

Studies using equivalent widths (EWs) and EW ratios to determine the spectral type of a star or stellar population have been pursued by several groups (e.g., Origlia, Moorwood, & Oliva 1993; Ali et al. 1995; Förster Schreiber 2000; and sources therein). Of particular interest to us is the work of Förster Schreiber (2000; hereafter FS), who examined H and K-band absorption lines to find temperature and luminosity indices and indices sensitive to dilution of the stellar spectrum by other sources. FS was primarily interested in spectral trends in giant and supergiant stars as the dominant stellar source in extragalactic NIR spectra, but his analysis includes some dwarf stars as well.

For comparison, we calculated the EWs of several prominent stellar absorption lines in the time-averaged spectrum of A0620-00 to compare to the spectral indices in FS. Table 2 gives the measured EWs. The lines were chosen to correspond to those in Table 3 of FS and were calculated using the same continuum normalization and integration limits. Where applicable, we also applied the EW correction for spectral resolution from Equations 2 – 4 of FS. The error bars on the EWs are the standard deviation of the mean for several measurements of each line with variable estimates of the continuum placement.

We first compared our EWs to the spectral indices given in Figure 5 of FS, which presents temperature and luminosity indicators for stars with solar or near-solar abundances. With the exception of Si I λ1.59 μm and Mg I λ2.28 μm, all of the lines under analysis show a strong trend of increasing EWs with decreasing stellar temperature. The EWs in A0620-00 are on the low side of the distributions for these lines, indicating stellar temperatures of $\geq$5000 K.

We also compared our EWs with those presented in Ali et al. (1995), who concentrated on temperature indices for dwarf stars. Note that the EWs in Table 2 used to compare to the Ali et al. (1995) indices are larger than those used for the FS indices because Ali et al. used a wider wavelength interval for their measurements, which we mirrored. Using their EW-temperature relationships, we obtain a temperature of 4600±300 K from Ca I and 5000±450 K from Na I. Therefore, if uncorrected for dilution, EWs in A0620-00 point to a donor star of roughly type K3V star or earlier. However, stars of spectral type K7V or earlier exceed the observed spectrum of A0620-00 in J and H when zero dilution is assumed in K. Therefore, we conclude that a diluting continuum source must be present in the NIR spectrum of A0620-00.

The amount of dilution of the stellar spectrum by another source is determined in FS by comparing the line ratios of adjacent atomic and molecular features (their Table 8). Unfortunately, their line ratios use the H and K band CO molecular absorption features, which we have already seen are not normal in A0620-00. Indeed, a comparison of the ^{12}CO 1.62 μm and 2.29 μm features in A0620-00 gives a result so disproportionately strong in the 1.62 μm line that the ratio doesn't even appear on the FS spectral index plot. Similarly, a comparison of the 2.29 μm feature to the nearby Na I and Ca I EWs indicates that the CO feature is weaker in A0620-00 than in any of the dwarf stars analyzed by FS. These results indicate that the CO features cannot be used to estimate the non-stellar dilution component A0620-00.

3.2. Fitting Spectral Type Standard Stars to the Spectrum of A0620-00

In an effort to quantify the contribution of the donor star to the NIR spectrum of A0620-00 and its dilution by other sources, we compared its spectrum to those of K3V, K5V, and K7V spectral type standard stars. The standard stars (listed in Table 1) were observed with the same instrument configuration and calibrated using the same procedures as for the A0620-00 observations. Before comparing the A0620-00 and template spectra, both were boxcar-smoothed over 3 pixels (one resolution element). The spectrum of A0620-00 was also dereddened with E(B–V) = 0.39 (using the reddening curve of Cardelli, Clayton, & Mathis (1989) and the standard star spectra were convolved with a Gaussian of 83 km s^{-1} FWHM to mimic the rotational broadening of the donor star in A0620-00 (Marsh, Robinson & Wood 1994). Note, however, that the rotational broadening is smaller than the 250 km s^{-1} resolution of the spectra and has a minimal effect on the results.

We wrote an IDL program to fit scaled template spectra to the spectrum of A0620-00 using the following steps. First, we selected a small wavelength range (typically, 0.1 μm or smaller) and fit a spline function to the continuum. The continuum points were selected by eye. After normalizing both the spectrum of A0620-00 and that of the template star and placing both spectra on a common, linear dispersion, we multiplied the template spectrum by a fraction, f, which represents the donor star contribution to the spectrum of A0620-00, and subtracted the scaled donor star spectrum from that of A0620-00. We varied f from 0 to 1 in increments of 0.01 to find the fraction that minimized the rms of the residual in each waveband. Finally, we repeated this analysis over several spectral lines and groups of lines over the full NIR spectral range. The fit regions we examined are given in Table 3. The resulting best values of f and the rms for each fit region and template spectrum is given in Table 4.

There are few absorption lines in the J band that are both relatively strong and uncontaminated by emission lines in the A0620-00 spectrum, so our fits were restricted to the portion of the long J band between Pγ and Pβ (1.10 – 1.26 μm). This region contains a blend of singly-ionized atomic species, including transitions of Mg I, Fe I, and Si I. The best fit fractions range from 0.78 to 1.0. There is a disparity between the strongest line in this range, Mg I λ1.183 μm and the other lines in this band: the Mg I line is best fit at $f \sim$0.9, but the other lines are weaker in the template than in A0620-00 even at f = 1.

The situation is less ambiguous in the H band. The best fit to the full H band spectrum using the K5V standard star is shown in Figure 6. The fit has f = 0.76 and an rms of 0.016. Although the χ^2 statistics are relatively poor ($\chi^2_\nu = 13.5$), there is a good qualitative correspondence between the morphologies of the observed and template spectra. Similar results are obtained with the K3V and K7V templates. Many of the stronger transitions (predominately Mg I and Si I lines) are too weak in the f = 0.76 template, however. If we restrict the fits to narrower regions around these lines, we generally obtain higher f and better fits (e.g., $\chi^2_\nu = 5.2$ for the 1.48 – 1.52 μm region fit by the K5V template).

The large χ^2_ν values for our fits indicate that our error bars are undersized relative to the true uncertainty in the fits. This is unsurprising, given the systematic uncertainties that affect modeling of NIR spectra in faint compact binaries, including the influence of sky background and telluric absorption correction, uncertain placement of the continuum level where no true continuum exists, and complex line blending wherein small temperature and/or abundance variations between the template and target stars can affect fit results. As a result, we have chosen to determine the mean value and uncertainty in the H-band donor star contribution by using an average of fits to multiple lines and multiple templates over the full waveband, rather than thorough the use of χ^2 statistics, as we believe the scatter between line fits provides a more rigorous sampling of uncertainties, particularly systematics. We determined the best representative value for the H band donor star contribution by averaging the best-fit f values for the three narrowband H fit regions (1.48 – 1.52 μm, 1.56–1.61 μm, and 1.70–1.72 μm) and the K5V and K7V templates. Averaging these values for the K5V and K7V template stars gives a donor star fraction $f = 0.82 \pm 0.02$.

In K, we fit three regions: the spectrum shortward of He I $\lambda 2.058$ μm, which is dominated by Ca I absorption lines; the region between He I and Bγ, which includes transitions of Mg I, Al I, and Si I; and the region longward of Bγ, which contains a rich blend of features, including transitions of Na I, Ca I, Fe I, Ti I, Mg I, and CO. Note that we do not have any fit results for the K3V template to the K-band spectrum, because the absorption lines in the K3V template are too weak relative to those of A0620-00, even at f=1. We have already shown from the comparison of the SEDs of A0620-00 and a K3V star that a star this hot cannot be the sole emission source (i.e., have $f = 1$) in A0620-00 in K without exceeding the observed spectrum at shorter wavelengths. Now we see that a K3V star also cannot be reconciled to the spectrum of A0620-00 by decreasing its fractional contribution, because its absorption lines are already too weak at $f = 1$ to match those observed in A0620-00. As a result, we restrict our fits in K to K5V and K7V templates.

The Ca I lines from 1.90 – 2.02 μm could not be simultaneously fit by a single value for f. The fit values given in Table 4 appear to the eye to be overdiluted as a result of spurious features (residuals of the telluric absorption correction) driving the fits. The strongest lines — 1.978 and 1.987 μm — are fit by $f \sim 0.5$, but at this value the other lines in this region are too weak. This spectral region may be contaminated by Bδ $\lambda 1.945$ μm emission from the accretion disk. Problems also beset the spectral fits in the 2.07 – 2.15 μm region. The K5V and K7V stellar spectra have anomalous emission bumps at 2.14 μm that cause visibly overdiluted fits over the full wavelength range. If the fits are restricted to 2.07 – 2.13 μm, best fits are obtained for $f \sim 0.65$, while fits to the strongest feature alone, Al I 2.117 μm, gives $f = 0.75$ for both the template fits.

The final fit region was the long-K portion of the spectrum, 2.18 – 2.42 μm, which includes numerous atomic species transitions and the CO bandheads. Figure 7 shows the best fits for the K5V template over the full fit region and when the fit is restricted to $\lambda < 2.28$ μm, excluding the region dominated by the CO lines. When long K is fit in its entirety, the fits are driven to large dilutions of the donor star to match the weak CO absorption in the A0620-00 spectrum. At these low donor fractions ($f = 0.45$ for the K5V template and $f = 0.37$ for the K7V template), the atomic lines are too weak in the template spectrum relative to those in A0620-00. If the fit is restricted to 2.18 – 2.28 μm, the donor fractions rise to $f = 0.81$ (K5V) and $f = 0.76$ (K7V). At these values, the atomic absorption spectrum of A0620-00 is well fit although there remain discrepencies between template and target spectra, most notably in the red components of Na I $\lambda 2.209$ and $\lambda 2.339$ μm and in the Fe I lines from 2.226 – 2.247 μm, all of which are too weak in the template relative to A0620-00. A single discrepancy in Fe I may explain these deviations, as there are Fe I transitions coincident with both of the "Na I" lines (see Figure 6 of FS for an illustration of the complex line blending in this spectral region).

3.3. Fitting Model Spectra to the Spectrum of A0620-00

In addition to modeling A0620-00 with standard star spectra, we used the LinBrod program to generate synthetic spectra for a Roche lobe-filling star in a compact binary with the geometry of A0620-00 (Bitner & Robinson 2006). We adopted the following parameter values for the models: P_{orb} = 0.323 d, q = 0.067, i = 41°, and K_2 = 433 km s^{-1} (McClintock & Remillard 1986; Marsh, Robinson & Wood 1994; Gelino et al. 2001). We created phase-resolved spectra for donor star temperatures of T = 4000, 4250, 4500, 4750, and 5000 K. Finally, we also created models at each temperature in which the carbon abundance in the star was reduced to [C/H] = -0.5, -1.0, -1.5, and -2.0. To compare to the observed spectrum of A0620-00, we averaged the model spectra over the binary orbit after removing the donor star orbital motion and smoothed the spectra to the observed spectral resolution.

Because the SED and spectral type standard star fits to the A0620-00 spectrum point to a donor star spectral type later than K3V, or $T < 5000$ K, we concentrated on the T = 4000, 4250, and 4500 K models. In an effort to characterize the carbon depletion required to match the observed CO line depths, we also focused on the long-K portion of the spectrum (2.18 – 2.42 μm) . Table 5 gives fit results for the LinBrod model fits. We first fit the solar abundance models and then repeated the fits for the carbon-depleted spectra. Figure 8 shows the normalized long K spectrum of A0620-00 with the solar abundance, T = 4000 K model and with the T = 4000 K, [C/H] = -1.5 spectrum. The model spectra has been scaled by f = 0.77, the best fit donor fraction for the 2.18 – 2.28 μm region. The [C/H] = -1.5 models provided the best fit to the spectrum of A0620-00 for all three of the donor temperatures examined (χ^2_ν = 4.0 for the T=4000 K, [C/H] = -1.5 model fit to 2.28 – 2.39 μm, versus χ^2_ν = 5.9 and χ^2_ν = 5.2 for the [C/H] = -1.0 and -2.0 models, respectively). The -0.5 and -1.0 models had CO lines that were still too strong relative to those of A0620-00, while the CO features were virtually absent in the -2.0 models and too weak to match the observed spectrum.

4. Discussion and Conclusions

4.1. The Donor Star in A0620–00

4.1.1. The Donor Star Spectral Type and Fractional Contribution to the NIR Spectrum

Our analysis of the NIR spectrum of A0620-00 has demonstrated three principal results: 1) the donor star is not the only NIR flux source, with 18±2% of the H-band flux originating in another component of the binary; 2) the donor star must be later than a K3V spectral type; and 3) the CO absorption lines are anomalously weak, requiring a carbon abundance of [C/H] = -1.5 in the donor star to match the observed line depths.

A comparison of the broadband NIR SED of A0620-00 with those of spectral type standard star spectra shows that the donor star cannot be the sole source of NIR flux. If the standard star spectra are normalized to the dereddened spectrum of A0620-00 in the K-band, they exceed the observed flux in the J and H wavebands. This result is true for all standard star spectra earlier than M0V. The discrepancy cannot be reconciled by changes in the differential reddening correction because the relative reddening correction between K and J and H is too small. Additionally, the K-band absorption lines in the K3V standard star are too weak to match the line depths seen in the A0620-00 spectrum even at a 100% donor star contribution. Decreasing the donor star contribution to $f < 1$ will only make the template lines weaker, so a K3V spectral type for the donor star is ruled out.

The most precise measurement of the donor star temperature is by González Hernández et al. (2004), who fit synthetic spectra created from model atmospheres to the visible spectrum of A0620-00. They found that $T_2 = 4900 \pm 100$ K, which corresponds to a K2/K3V spectral type. This result is not in agreement with our requirement that the donor star be later than K3V. There are reasons to believe that the González Hernández et al. (2004) results may be unreliable, however. To determine the stellar parameters they used 24 Fe I lines, to which they fit models with five free parameters: stellar temperature, gravity, and metallicity, as well as a normalization and slope to represent dilution from the accretion disk. The use of Fe I lines alone to constrain all stellar parameters (plus the disk contribution) is uncommon practice for stellar modeling, which typically relies on independent determinations of the stellar temperature, as well as on both Fe I and Fe II transitions. González Hernández et al. (2004) also determined that the abundances of the elements they fit were slightly above solar values. The adoption of a cooler donor star temperature, as required by our results, will reduce their derived abundances.

We conclude that the spectral type of the donor star is most likely between K5V to K7V, but do not attempt to constrain the spectral type more precisely. The rms values for the dilution fits to various regions of the A0620-00 spectrum are comparable for both spectral types and we cannot rely on the CO features to create more precise temperature indices. We therefore averaged the dilution values from both spectral type fits for the three narrow regions in the H-band to derive our H-band donor star fraction: $f = 0.82 \pm 0.02$, or an 82% donor star contribution in H. The donor fraction in long K ($> 2.2\mu$m) is 81% for a K5V template or 76% for the K7V. Figure 9 shows the spectrum of A0620-00 with a K5V template star scaled to 82% of the H-band flux and the A0620-00 spectrum after the contribution of the donor star has been subtracted. While the spectrum of A0620-00 is dominated by the K type donor, there is a significant second component consisting of a blue continuum and strong H I and He II line emission.

Our results of a K5V to K7V donor star spectral type and 18% – 24% veiling in H and K do not agree with those of Gelino et al. (2001), who found that the NIR SED of A0620-00 matched that of a K4V (T = 4600 K) star with no dilution. As pointed out by Hynes et al. (2005), however, there is a degeneracy between the spectral type of the star and the amount and distribution of a veiling spectrum in an XRB: a cooler donor star plus a diluting component can result in the same SED as a hotter donor star with no contamination. Hynes et al. showed that even a 100 K overestimate of the temperature of the donor star could result in a factor of two underestimate of the veiling. Because our data show, both in the line EWs and the NIR SED, that a K type donor star cannot be the only NIR flux source, we conclude that Gelino et al. (2001) overestimated the temperature of the donor star and consequently underestimated the spectral dilution in the NIR.

Our results also disagree with the recent work of Harrison et al. (2007), who argue by analogy with the IR spectrum of the cataclysmic variable SS Cygni that A0620-00 has <4% dilution in the K-band. Their argument can be summarized as follows: a) A0620-00 and SS Cyg have similar K-band spectral slopes, binary properties, and quiescent mass accretion rates; b) SS Cyg also has a mid-IR excess; c) the NIR and MIR SEDs of SS Cyg can be well fit by a K4V stellar spectrum plus free-free emission; d) because A0620-00 and SS Cyg are similar, application of the star plus wind model can be extended from the latter to the former to estimate a ∼4% limit on the contamination level of the NIR spectrum of A0620-00.

We have several concerns about this line of reasoning. First, as already discussed above, the similarity of a SED to that of a field star does not preclude contaminating emission from the disk. The data shown in Harrison et al. reinforce this: the JHK colors of SS Cyg are consistent with that of an undiluted K4V star even as the ellipsoidal light curves show clear evidence of contamination. In fact, Harrison el al. point out that the K-band spectrum of A0620-00 has a different slope from those of the field stars, which provides fairly clear evidence of contamination. Second, it is not known whether free-free emission is the correct explanation for the excess MIR flux observed in SS Cyg. Another possibility discussed by Dubus et al. (2004), who originally published the IR SED shown by Harrison et al., is that circumbinary disk emission is responsible. Indeed, Muno & Mauerhan (2006) have found a MIR component in A0620-00, which they fit with a $\simeq$600 K blackbody component, consistent with emission from circumbinary dust rather than free-free emission in a wind. The cool blackbody component found by Muno & Mauerhan (2006) does not affect the NIR spectrum of A0620-00, which suggests that the attempt to use MIR data from SS Cyg to estimate the NIR contamination in A0620-00 is a red herring. Finally, we reiterate what our simultaneous, JHK spectra of A0620-00 indicate directly about the donor star contamination in the system: based on the shape and fluxes of the JHK continuum spectrum, the absolute EWs of the atomic absorption lines, and dilution analyses using both field stars and a Roche-lobe filling model spectrum, the donor star must be significantly diluted ($\sim$20%), even in the K-band.

4.1.2. Weak CO Features in the Donor Star Spectrum

Although the atomic absorption line spectrum in A0620-00 is consistent with a K5V – K7V spectral type, the molecular ^{12}CO lines are significantly weaker in A0620-00 than in a field star, corresponding to CO line strengths normally seen in early G stars. Using the LinBrod model spectra of a Roche lobe-filling star, we found that reducing the C abundance to [C/H] = -1.5 results in a better match to the CO lines in the spectrum than the [C/H] = 0, -1.0, and -2.0 models when the donor star fraction is fit to f = 0.77.

The weakness of the ^{12}CO lines in A0620-00 has already been noted by Harrison et al. (2007), who determine that the ^{12}C abundance must be decreased 50% to match the depth of the ^{12}CO bandheads. The 50% reduction in ^{12}C abundance ([^{12}C/H] = -0.3) found by Harrison et al. is significantly smaller than the 97% drop we claim. Again, however, we have several concerns about the method by which Harrison et al. obtained their results. First, they started with the line list included in the spectral synthesis program SPECTRUM (Gray & Corbally 1994), but when they were unable to match the spectra of standard spectral type field stars using this line list (and Kurucz atmospheres) due to the presence of strong absorption features in the model but not the observed spectra, they abandoned it and constructed one consisting only of Na I, Mg I, and CO transitions. When they found that the lines in their new models were too weak to match those of field stars at the correct temperature, they globally increased the log(gf) values of every line in their new line list to match up with observations. They then applied this revised model to the spectrum of A0620-00, adjusting the C isotopic abundances until the best fit by eye was achieved.

We are not confident in the quantitative reliability of spectral model fits in which spectral lines have been dropped and oscillator strengths altered in order to achieve even a rough fit to a K5V field star. We note in contrast that our LinBrod models give fits to the spectrum of A0620-00 of comparable quality of those using template field stars with no deletions or alterations to the spectral synthesis line lists required. Our other concern with the Harrison et al. fits is the placement of the continuum and evaluation of the best model fit. They determined the best-fit model by eye. To our eyes, however, the fits they show in their Figure 3 do not properly take into account the actual data quality: their pseudo-continuum levels appear too high and their CO line minima are too low in their preferred model. A rough comparison of their observed spectrum to ours shows that the ^{12}CO normalized line depths are similar in both data sets, suggesting that a statistical model fit to their spectrum would result in a ^{12}C abundance similar to the one we obtain.

Finally, Harrison et al. contend that in addition to a low ^{12}C abundance in A0620-00, the ^{13}C abundance is enhanced, such that ^{13}C/^{12}C = 1. They base their identification of ^{13}CO on the presence of a feature coinciding with the ^{13}CO(3,1) 2.374 μm bandhead. However, they also note that the ^{13}CO(2,0) 2.345 μm is not seen in their spectrum, despite being the stronger feature of the two. Given the poor atmospheric conditions at the time their data was taken and the increasing amount of telluric H_20 absorption at these wavelengths, we do not believe that their data provide a clear detection of ^{13}CO and certainly not of ^{13}C at equal abundance with ^{12}C. In our spectrum of A0620-00, there is a feature at the location of the ^{13}CO(2,0) 2.345 μm bandhead, but no feature coinciding with ^{13}CO(3,1) 2.374 μm. We have marked the locations of the first two ^{13}CO bandheads in our Figure 4. Dhillon et al. (2002) point out, however, that a Ti I feature is coincident with the ^{13}CO(2,0) 2.345 μm bandhead and is a much more likely explanation of the feature we see. As a result, we do not believe that an unambiguous detection of ^{13}CO can be made in our spectrum and we find no evidence of any enhancement of this species in A0620-00.

Anomalously weak CO absorption features have been seen in other compact binary systems. The NIR spectra of several cataclysmic variables show weak or absent ^{12}CO absorption (Harrison et al. 2000, 2004). In the dwarf nova U Gem, the NIR CO absorption lines are significantly weaker than in the M3V standard star spectrum that provides a good match to the atomic lines. Model fits to the FUV spectrum of the metal-enriched white dwarf in U Gem show that the C abundance on the WD surface is [C/H] = -1.0, while the N abundance is highly super-solar, [N/H] = 0.7 (Sion et al. 1998; Long & Gilliland 1999; Froning et al. 2001). Similarly, in the UV spectrum of the BH XRB XTE J1118+480 in outburst, typically strong emission lines of C IV and O V are undetectable, while the N V λ1240 Å appears enhanced (Haswell et al. 2002). The UV line ratios are inconsistent with photoionization models, leading Haswell et al. to conclude that the emission spectrum is indicative of the accretion of C-depleted material from the donor star. As a result, A0620-00 can be added to the ever-increasing list of cataclysmic variables and XRBs that show depleted C (and, in some cases, enhanced N), pointing to a common history of nuclear processing of C to N in compact binary systems.

4.2. The Mass of the Black Hole in A0620–00

Based on previous work, the mass of the BH in A0620-00 is known to the value of one unknown, the binary inclination: $M_1 = (3.09 \pm 0.09) \sin^{-3} i$ (Marsh, Robinson & Wood 1994). The orbital inclination can be obtained by modeling the light curve of the donor star. The donor star fills its Roche lobe and is distorted in shape, which leads to a double-humped ellipsoidal variation in the light curve, the amplitude of which is dependent on inclination. If a source besides the donor star contributes to the light curve, the amplitude of the ellipsoidal variation will be diluted, leading to an underestimate of the inclination and a corresponding overestimate of the BH mass if the contaminating source is not taken into account.

The most precise inclination results to date were reported by Gelino et al. (2001), who modeled JHK light curves of A0620-00. Based on good agreement between the target SED and that of a dereddened K4 star, they concluded that the donor star is the only NIR continuum source in A0620-00. Using this assumption, they modeled the ellipsoidal light curve and found $i = 40\overset{\circ}{.}75 \pm 3^{\circ}$ and $M_1 = 11.0 \pm 1.9\ M_{\odot}$. As discussed above, however, the NIR SED alone is insufficient to resolve the degeneracy between donor star temperature and veiling by another flux source in the system. Our results indicate that the donor star cannot be the only NIR flux source in A0620-00 and that consequently, the Gelino et al. results overestimate the BH mass in A0620-00.

We previously modeled the H-band light curve in A0620-00 with a donor star plus accretion disk model and determined $38^{\circ} \leq i \leq 75^{\circ}$, or $3.3 \leq M_1 \leq 13.6\ M_{\odot}$ (Froning & Robinson 2001). The broad range of values was caused by a degeneracy between the inclination and the fractional contribution of the accretion disk to the H-band light. Table 5 of Froning & Robinson (2001) gives the inclination in A0620-00 as a function of the fractional contribution of diluting sources in the H-band. In § 3.2 of this paper, we determined that the donor star contributes 82±2% of the H-band flux in A0620-00. This result, a diluting fraction of 18±2%, combined with Table 5 in Froning & Robinson (2001) gives a binary inclination for A0620-00 of $i = 43 \pm 1^{\circ}$.

Based on this inclination, we obtain the mass of the BH accretor in A0620-00: $M_1 =$ 9.7±0.6 $M_{\odot}$. This result is comparable to previous estimates of the BH mass in the literature. Shahbaz, Naylor & Charles (1994) found a BH mass of 10 $M_{\odot}$, while Gelino et al. (2001)

found $M_1 = 11.0\pm1.9\ M_\odot$. The inclination we derive is within the error interval of Gelino et al. The difference in BH masses between the two results comes from the slightly higher inclination we adopt as a result of our determination that the donor star cannot be the sole NIR emission source.

The error bar on our derived BH mass represents the propagated statistical errors in the result. A potential source of systematic uncertainty is our assumption that the atomic absorption spectrum of A0620-00 can be modeled by template spectra with solar abundances. The fact that the C abundance in A0620-00 has to be decreased significantly to match the CO lines suggests the need for caution in this regard. However, the relative line ratios of the atomic transitions largely agree with each other in the derived fractional donor star contributions. These lines are also strong transitions that lie on the flat portion of the curve of growth and will not be sensitive to small abundance variations. Finally, we note that while González Hernández et al. (2004) derived slightly super-solar abundances for the metal lines in A0620-00, they used a stellar temperature that is too hot to be consistent with the NIR SED. The adoption of a cooler temperature for the donor star will cause the metal line abundances required to fit the optical spectrum to decrease.

Another potential source of systematic error is the large time interval (8 years) between acquisition of the NIR light curve and the spectra. Our analysis assumed that the donor star diluting fraction found by analyzing the spectra applies equally well to the light curve data. This assumption is valid, we believe, because while A0620-00 is variable, its NIR colors typically don't vary by more than 0.2 mag, and six observations of the H-band light curve spaced over days to years had mean colors that agreed to within 0.04 mag (Froning & Robinson 2001; Gelino et al. 2001). Our rough estimate of the absolute calibration of our time-averaged spectrum was also consistent with the previous measurements. We can estimate the uncertainty in the non-donor star contribution by assuming that it could vary by $\pm4\%$, consistent with the previous measurements. This would cause the donor star fraction to range from $79 \leq f \leq 86$, which results in $i = 43 \pm 1^\circ$, consistent with our statistical uncertainties.

We thank Nathaniel Cunningham for assistance in observing A0620-00, and the staff at the IRTF for their support. We also thank Chris Sneden and Niall Gaffney for their help in calculating the LinBrod donor star spectra and for useful discussions.

Facilities: IRTF(SpeX)

REFERENCES

Ali, B., Carr, J. S., Depoy, D. L., Frogel, J. A., & Sellgren, K. 1995, AJ, 110, 2415

Bailyn, C. D., Jain, R. K., Coppi, P., & Orosz, J. A. 1998, ApJ, 499, 367

Bitner, M. A. & Robinson, E. L. 2006, AJ, 131, 1712

Cardelli, J. A., Clayton, G. C., & Mathis, J. S. 1989, ApJ, 422, 158

Cushing, M. C., Vacca, W. D., & Rayner, J. T. 2004, PASP, 116, 362

Dhillon, V. S., Littlefair, S. P., Marsh, T. R., Sarna, M. J., & Boakes, E. H. 2002, A&A, 393, 611

Dubus, G., Campbell, R., Kern, B., Taam, R. E., & spruit, H. C. 2004, MNRAS, 349, 869

Elvis, M., Page, C. G., Pounds, K. A., Ricketts, M. J., & Turner, M. J. L. 1975, Nature, 257, 656

Förster Schreiber 2000, AJ, 120, 2089

Froning, C. S., Long, K. S., Drew, J. E., Knigge, C., & Proga, D. 2001, ApJ, 562, 963

Froning, C. S., & Robinson, E. L. 2001, AJ, 121, 2212

Fryer, C. L. & Kalogera, V. 2001, ApJ, 554, 548

Gelino, D. M. & Harrison, T. E. 2003, ApJ, 599, 1254

Gelino, D. M., Harrison, T. E., & Orosz, J. A. 2001, AJ, 122, 2668

González Hernández, J. I., Rebolo, R., Israelian, G., Casares, J., Maeder, A., & Meynet, G. 2004, ApJ, 609, 988

Gray, R. O. & Corbally, C. J. 1994, AJ, 107, 742

Harrison, T. E., Howell, S. B., Szkody, P., & Cordova, F. A. 2007, AJ, 133, 162

Harrison, T. E., Osborne, H. L., & Howell, S. B. 2005, AJ, 129, 2400

Harrison, T. E., Osborne, H. L., & Howell, S. B. 2004, AJ, 127, 3493

Harrison, T. E., McNamara, B. J., Szkody, P., & Gilliland, R. L. 2000, AJ, 120, 2649

Haswell, C. A., Hynes, R. I., King, A. R., & Schenker, K. 2002, MNRAS, 332, 928

Haswell, C. A., Robinson, E. L., Horne, K., Stiening, R. F. & Abbott, T. M. C. 1993, ApJ, 411, 802

Hynes, R. I., Robinson, E. L., & Bitner, M. 2005, ApJ, 630, 405

Kleinmann, S. G. & Hall, D. N. B. 1986, ApJ, 62, 501

Leibowitz, E. M., Hemar, S., & Orio, M. 1998, MNRAS, 300, 463

Long, K. S. & Gilliland, R. L. 1999, ApJ, 511, 916

Marsh, T. R., Robinson, E. L. & Wood, J. H. 1994, MNRAS, 266, 137

McClintock, J. E. & Remillard, R. A. 2005, in Compact Stellar X-ray Sources, eds. W. Lewin & M. van der Klis, (Cambridge: Cambridge University Press), in press

McClintock, J. E. & Remillard, R. A. 1986, ApJ, 308, 110

McClintock, J. E., Petro, L. D., Remillard, R. A. & Ricker, G. R. 1983, ApJL, 266, L27

Meyer, M. R., Edwards, S., Hinkle, K. H., & Strom, S. E. 1998, ApJ, 508, 397

Muno, M. P. & Mauerhan, J. 2006, ApJ, 648, L135

Oke, J. B. 1977, ApJ, 217, 181

Origlia, L., Moorwood, A. F. M., & Oliva, E. 1993, A&A, 280, 536

Orosz, J. A., Bailyn, C. B., Remillard, R. A., McClintock, J. E. & Foltz, C. B. 1994, ApJ, 436, 848

Rayner, J. T., Toomey, D. W., Onaka, P. M., Denault, A. J., Stahlberger, W. E., Vacca, W. D., Cushing, M. C., & Wang, S. 2003, PASP, 115, 362

Shahbaz, T., Hynes, R. I., Charles, P. A., Zurita, C., Casares, J., Haswell, C. A., Araujo-Betancor, S., & Powell, C. 2004, MNRAS, 354, 31

Shahbaz, T., Bandyopadhyay, R. M. & Charles, P.A. 1999, A&A, 346, 82

Shahbaz, T., Naylor, T. & Charles, P. A. 1994, MNRAS, 268, 756

Sion, E. M., et al. 1998, ApJ, 496, 449

Vacca, W. D., Cushing, M. C., & Rayner, J. T. 2003, PASP, 115, 389

Wallace, L., Meyer, M. R., Hinkle, K., & Edwards, S. 2000, ApJ, 535, 325

Wu, C.-C., Aalders, J. W. G., van Duinen, R. J., Kester, D., & Wesselius, P. R. 1976, A&A, 50, 445

e

Table 1. SpeX Observations

Object	Date (UT)	Instrument	T_{exp} (min)	Φ[a]
A0620-00	2004 Jan 8	SpeX	290	0.59 – 1.47
A0620-00	2004 Jan 9	SpeX	280	0.69 – 1.49
A0620-00	2004 Jan 10	SpeX	250	0.92 – 1.61
HD42606 (K2.5 III)	2004 Jan 18	SpeX	1.2	···
HD 3765 (K2 V)	2004 Jan 18	SpeX	2	···
HD16160 (K3 V)	2004 Jan 19	SpeX	1.8	···
61 Cyg A (K5 V)	2000 Sept 15	SpeX	0.5	···
61 Cyg B (K7 V)	2000 Sept 15	SpeX	0.5	···

[a]Orbital phase coverage of A0620–00 for each night's observations, based on the ephemeris of McClintock & Remillard (1986).

Table 2. Equivalent Widths of Selected Absorption Lines

Feature	EW[a] (Å)	EW[b] (Å)
Si I 1.5892	1.52±0.04	···
^{12}CO (6,3) 1.6187	0.86±0.07	···
Na I 2.2076	0.94±0.06	2.18±0.04
Fe I 2.2263	0.36±0.05	···
Fe I 2.2387	0.40±	···
Ca I 2.2636	1.06±0.06	3.21±0.03
Mg I 2.2814	0.43±0.04	0.68±0.06
^{12}CO (2,0) 2.2935	0.38±0.06	2.26±0.08
^{12}CO (3,1) 2.3227	0.22±0.02	···
^{13}CO (2,0) 2.3448	0.64±0.04	···

[a]EWs calculated using the integration limits of Förster Schreiber 2000.

[b]EWs calculated using the integration limits of Ali et al. (1995).

Table 3. Wavelength Ranges for Spectral Fits

Waveband	λ Range (mum)	Description
J	1.10 – 1.26	Long J
	1.175 – 1.215	Blend incl. Mg I, Fe I, Si I
H	1.4 – 1.8	Full H band
	1.48 – 1.52	Mg1 lines.
	1.56 – 1.61	Blend incl. Mg I, Si I
	1.70 – 1.72	Mg1
K	1.90 – 2.02	Several Ca I lines.
	2.07 – 2.15	Short K incl. Mg I, Si I, Al I.
	2.18 – 2.42	Long K incl. CO bandhead.
	2.18 – 2.28	No CO, lines incl. Na I, Fe I, Ca I, Mg I.

Table 4. Template Star Fits to A0620–00 Spectrum

Template Spectral Type	Wavelength Range (μm)	Template Fraction (f)	rms
K3V	1.10–1.26	0.78	0.012
	1.175 – 1.215	0.82	0.010
	1.4–1.8	0.76	0.016
	1.48 – 1.52	0.71	0.011
	1.56 – 1.61	0.81	0.011
	1.70 – 1.72	0.91	0.009
K5V	1.10 – 1.26	0.90	0.013
	1.175 – 1.215	1.0	0.010
	1.4 – 1.8	0.78	0.016
	1.48 – 1.52	0.82	0.010
	1.56 – 1.61	0.88	0.015
	1.70 – 1.72	0.78	0.010
	1.90 – 2.02	0.37	0.02
	2.07 – 2.15	0.52	0.01
	2.18 – 2.42	0.45	0.012
	2.18 – 2.28	0.81	0.009
K7V	1.10 – 1.26	0.87	0.013
	1.175 – 1.215	0.99	0.011
	1.4 – 1.8	0.76	0.017
	1.48 – 1.52	0.82	0.010
	1.56 – 1.61	0.85	0.015
	1.70 – 1.72	0.77	0.009
	1.90 – 2.02	0.39[a]	0.021
	2.07 – 2.15	... [b]	...
	2.18 – 2.42	0.37	0.014
	2.18 – 2.28	0.76	0.009

[a]Fits too diluted due to noise in spectra.

[b]Fits compromised by spurious feature in template.

Table 5. LinBrod Fits to A0620–00 Spectrum

Model Temperature (K)	Model C Abundance ($\log[C/H]/[C/H]_\odot$)	Wavelength Range (μm)	Template Fraction (f)	rms
4000	0.0	2.18 – 2.28	0.72	0.011
4250	0.0	2.18 – 2.28	0.76	0.011
4500	0.0	2.18 – 2.28	0.99	0.011
Full Long K Region Including CO Lines				
4000	0.0	2.18 – 2.38	0.14	0.015
4000	-0.5	2.18 – 2.38	0.28	0.014
4000	-1.0	2.18 – 2.38	0.54	0.012
4000	-1.5	2.18 – 2.38	0.78	0.011
4000	-2.0	2.18 – 2.38	0.74	0.012
4250	0.0	2.18 – 2.38	0.14	0.015
4250	-0.5	2.18 – 2.38	0.28	0.014
4250	-1.0	2.18 – 2.38	0.56	0.013
4250	-1.5	2.18 – 2.38	0.82	0.012
4250	-2.0	2.18 – 2.38	0.81	0.012
4500	0.0	2.18 – 2.38	0.17	0.015
4500	-0.5	2.18 – 2.38	0.35	0.014
4500	-1.0	2.18 – 2.38	0.71	0.013
4500	-1.5	2.18 – 2.38	0.96	0.012
4500	-2.0	2.18 – 2.38	0.93	0.013
Longward of the 2.29 μm Bandhead Only[a]				
4000	-0.5	2.28 – 2.38	0.77	0.025
4000	-1.0	2.28 – 2.38	0.77	0.014
4000	-1.5	2.28 – 2.38	0.77	0.012
4000	-2.0	2.28 – 2.38	0.77	0.013
4250	-0.5	2.28 – 2.38	0.77	0.024

Table 5—Continued

Model Temperature (K)	Model C Abundance ($\log[C/H]/[C/H]_{\odot}$)	Wavelength Range (μm)	Template Fraction (f)	rms
4250	-1.0	2.28 – 2.38	0.77	0.014
4250	-1.5	2.28 – 2.38	0.77	0.012
4250	-2.0	2.28 – 2.38	0.77	0.013
4500	-0.5	2.28 – 2.38	0.77	0.020
4500	-1.0	2.28 – 2.38	0.77	0.014
4500	-1.5	2.28 – 2.38	0.77	0.013
4500	-2.0	2.28 – 2.38	0.77	0.014

[a]Donor star fraction fixed in these models to the best-fit value to the nearby atomic lines from the template star fits.

Fig. 1.— The NIR spectrum of A0620–00, obtained in 2004 January. The solid line shows the time-averaged spectrum of A0620. Individual exposures were shifted to remove the orbital motion of the donor star before averaging. The dotted line shows the spectrum after dereddening, assuming E(B–V) = 0.39 (Wu et al. 1976).

Fig. 2.— The spectrum of A0620-00 in J. Prominent spectral features are labeled. An error bar representative of the statistical uncertainty per resolution element is plotted on the far right of the plot. Also shown at the bottom of the figure is the spectrum of HD45137, the A0V star used for telluric correction of the A0620–00 spectra. The spectrum retains the throughput profile of each spectral order but is not shown with absolute flux calibration. The H I lines intrinsic to the A0V spectrum have been fitted and removed using the xtellcor program developed by the IRTF.

Fig. 3.— The spectrum of A0620-00 in H. Prominent spectral features are labeled. A representative error bar for a resolution element is plotted on the far right. The telluric spectrum is also shown at the bottom of the figure.

Fig. 4.— The spectrum of A0620-00 in K. Prominent spectral features are labeled. A representative error bar for a resolution element is plotted on the far right. The telluric spectrum is also shown.

Fig. 5.— Shown in black is the dereddened spectrum of A0620-00. Shown in gray is the spectrum of 61 Cyg A, a K5V spectral type star. The spectrum of 61 Cyg A has been normalized to the flux of A0620 just blueward of the ^{12}CO 2.29 μm bandhead.

Fig. 6.— The normalized H-band spectrum of A0620–00 with a scaled spectral type standard star fit. The standard star, shown in red, is 61 Cyg A, a K5V star. It has been scaled by $f = 0.76$.

Fig. 7.— The normalized K-band spectrum of A0620–00 with a scaled spectral type standard star fit. The template star is 61 Cyg A, a K5V star. The solid red spectrum shows the template scaled by $f = 0.45$, the best fit over the full 2.18 – 2.42 μm range. The dashed red spectrum shows the template scaled by $f = 0.81$, the best fit to the 2.18 − 2.28 μm region.

Fig. 8.— The normalized K-band spectrum of A0620–00 with scaled LinBrod T = 4000 K model spectra fits. The solid red line shows the LinBrod model with [C/H] = -1.5, while the dashed red line shows the solar abundance model. To avoid confusion, the latter is shown only for $\lambda > 2.288$ μm. The models are scaled by $f = 0.77$.

Fig. 9.— The top panel shows the dereddened spectrum of A0620-00 in black and the spectrum of 61 Cyg A, a K5V star, in gray. The spectrum of the K5V template has been

scaled to 82% of the A0620-00 flux at the center of the H band, 1.6 μm. The lower panel shows the NIR spectrum of the accretion disk in A0620-00, created by subtracting the template spectrum from that of A0620-00.

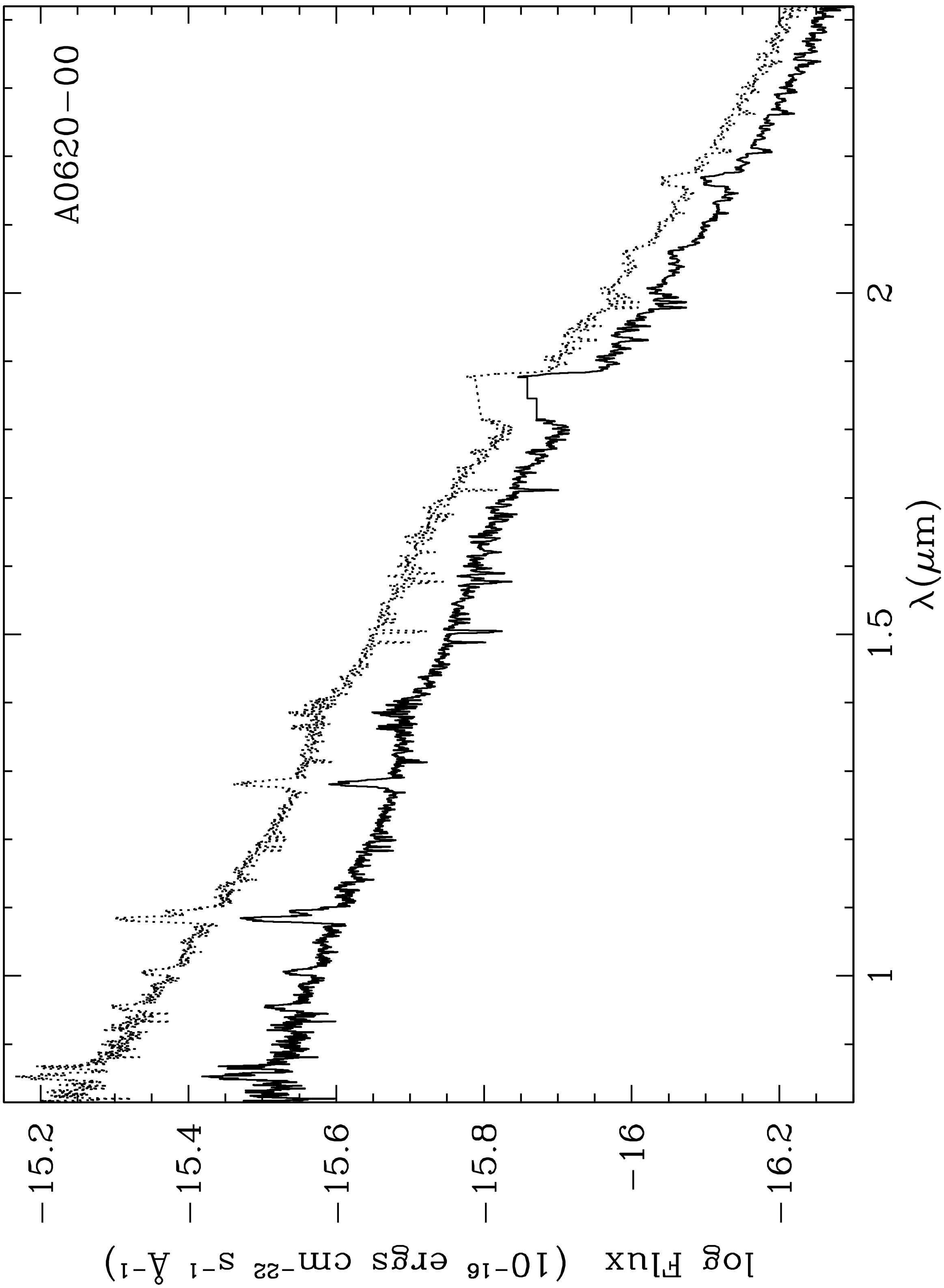

f1.eps

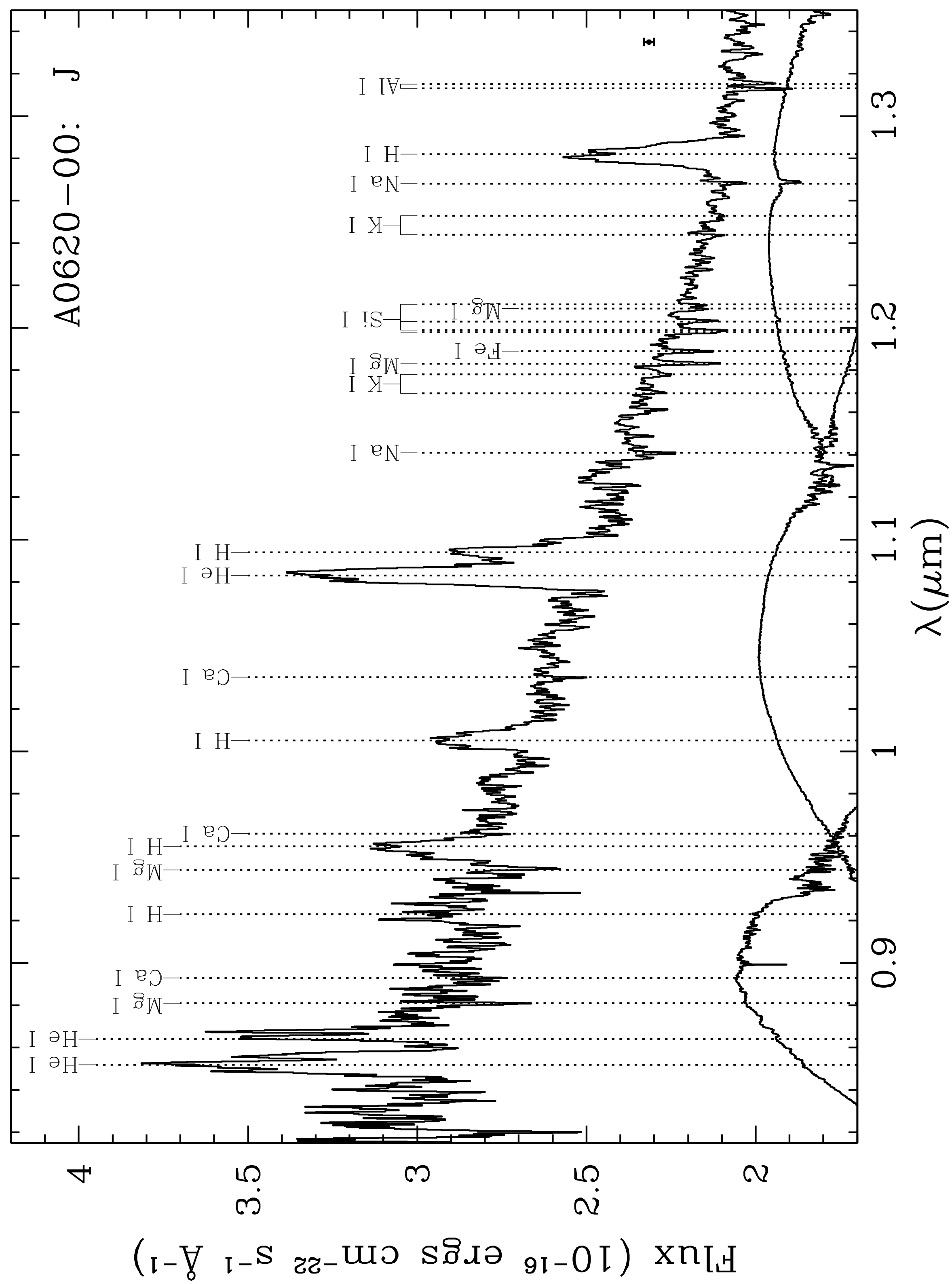

A0620−00: J
Flux (10-16 ergs cm-2 s-1 Å-1)
λ(μm)
He I
He I
Mg I
Ca I
H I
Mg I
H I
Ca I
H I
Ca I
He I
H I
Na I
K I
Mg I
Fe I
Si I
Mg I
K I
Na I
H I
Al I

f2.eps

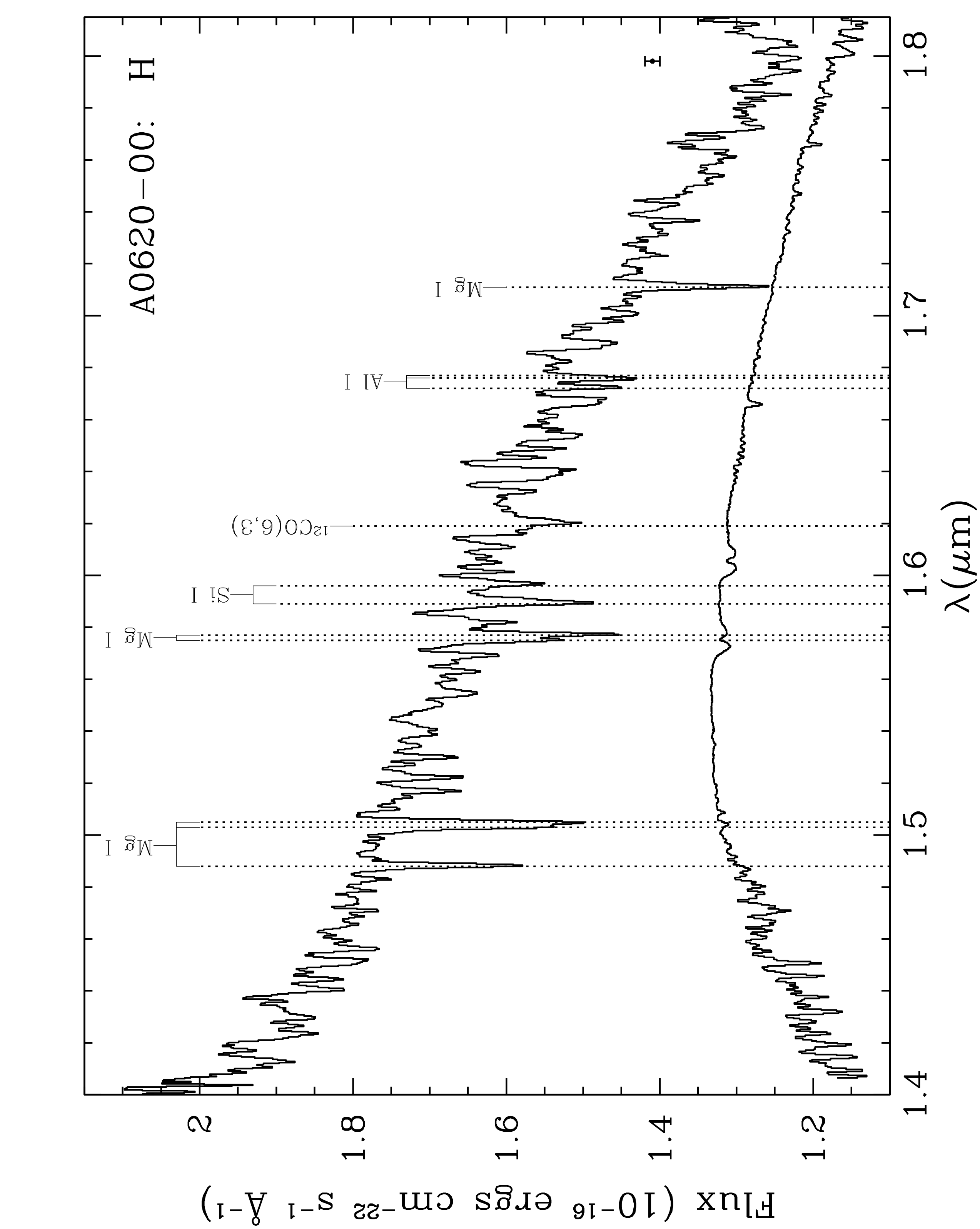

f3.eps

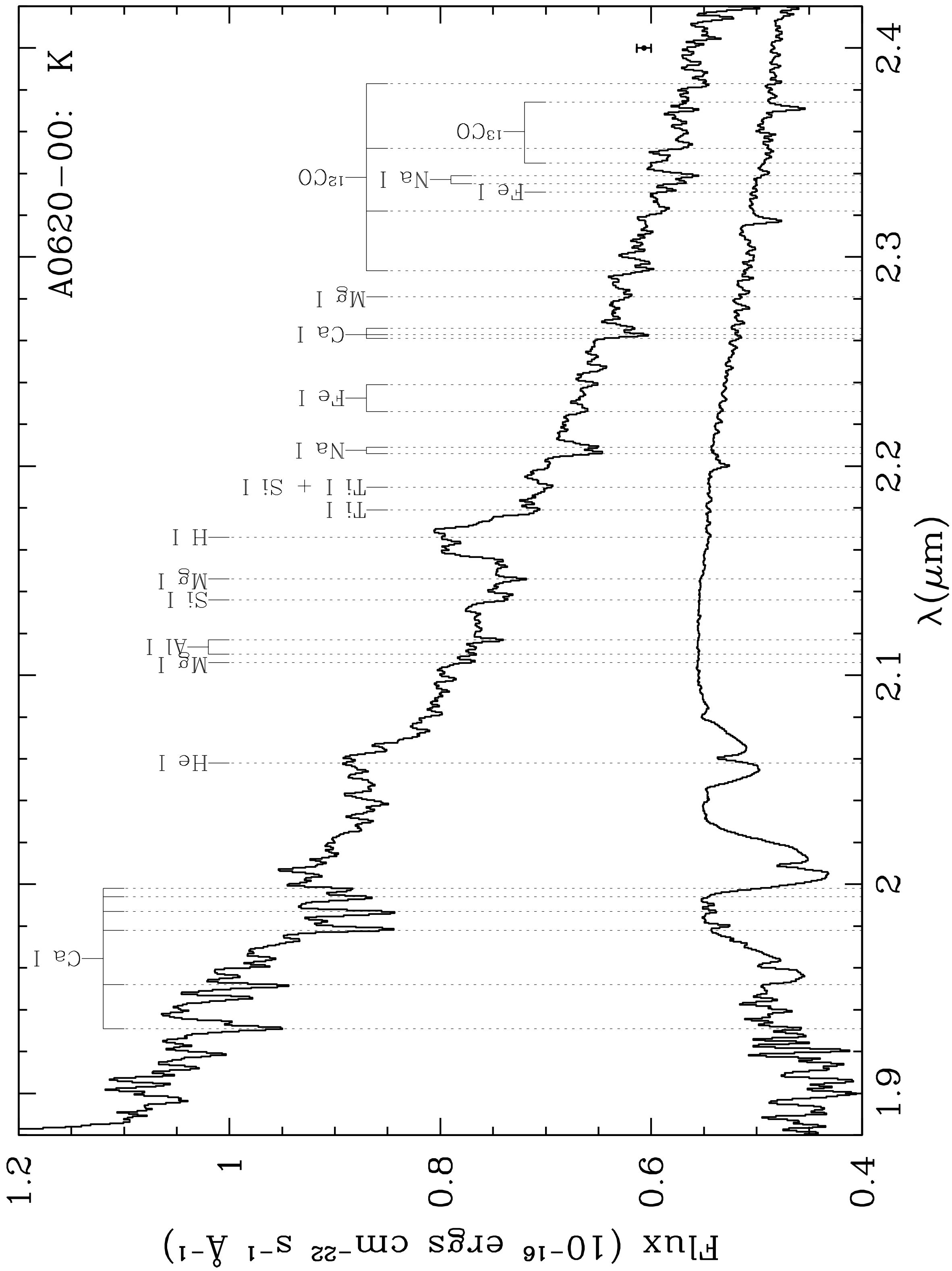
A0620−00: K
λ(μm)
Flux
Ca I
He I
Mg I
Al I
Si I
H I
Ti I
Ti I + Si I
Na I
Fe I
Ca I
Mg I
12CO
13CO

f4.eps

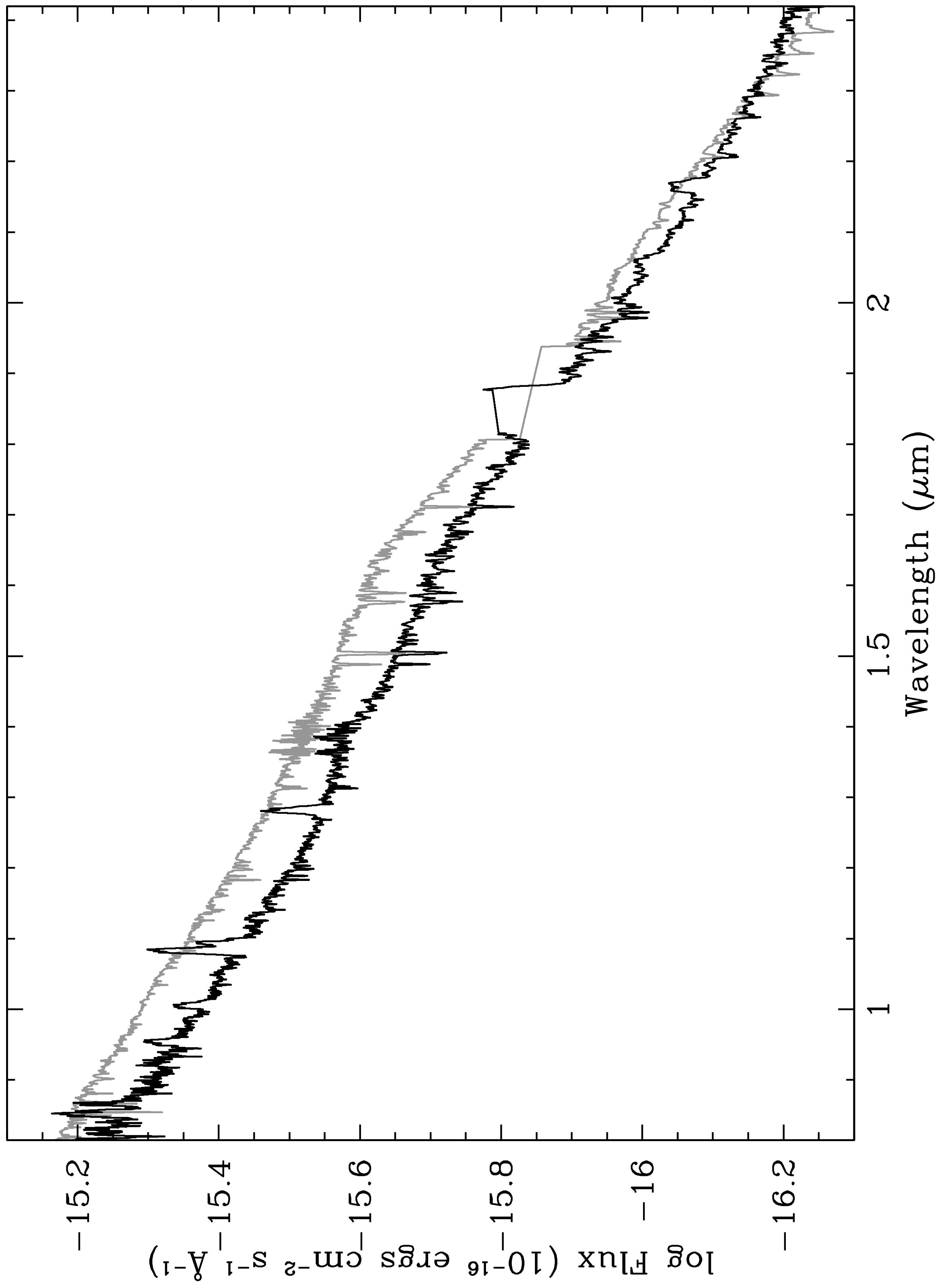

1
1.5
2
Wavelength (μm)
−15.2
−15.4
−15.6
−15.8
−16
−16.2
log Flux (10-16 ergs cm-2 s-1 Å-1)

f5.eps

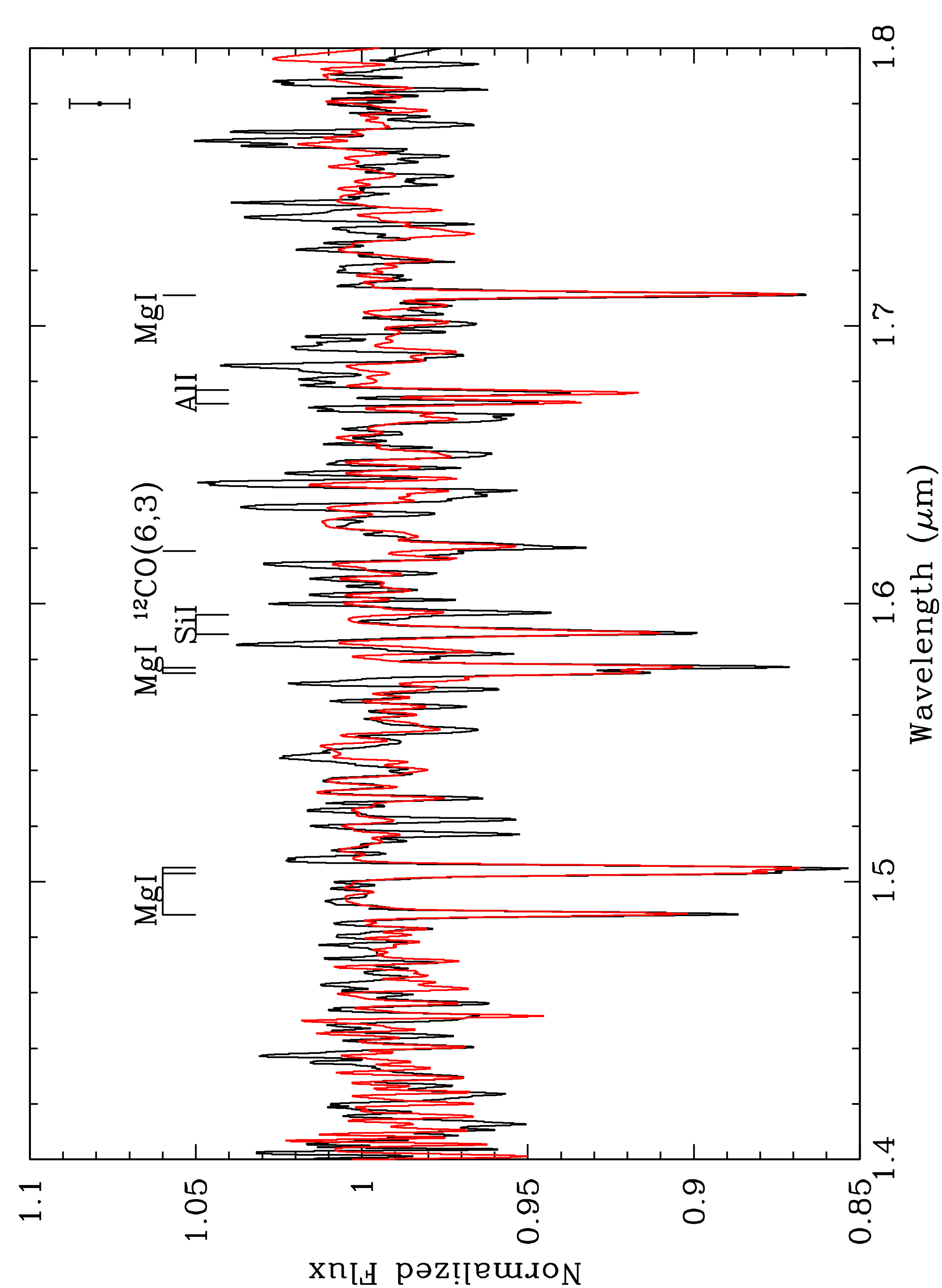
MgI
SiI
12CO(6,3)
AlI
MgI
Wavelength (μm)
Normalized Flux
1.4
1.5
1.6
1.7
1.8
0.85
0.9
0.95
1
1.05
1.1

f6.eps

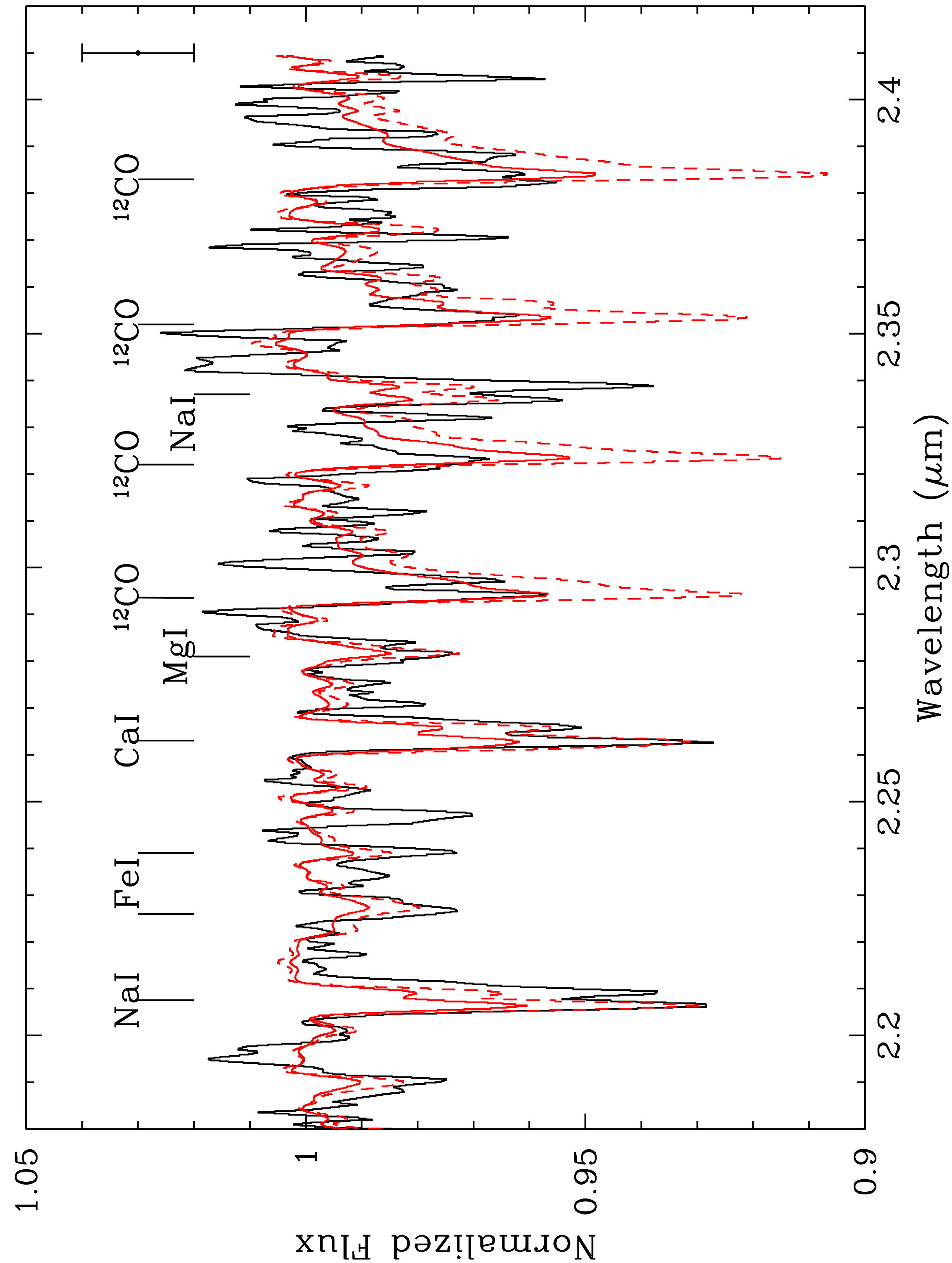
NaI
FeI
CaI
MgI
12CO
12CO
NaI
12CO
12CO
Normalized Flux
Wavelength (μm)
1.05
1
0.95
0.9
2.2
2.25
2.3
2.35
2.4

f7.eps

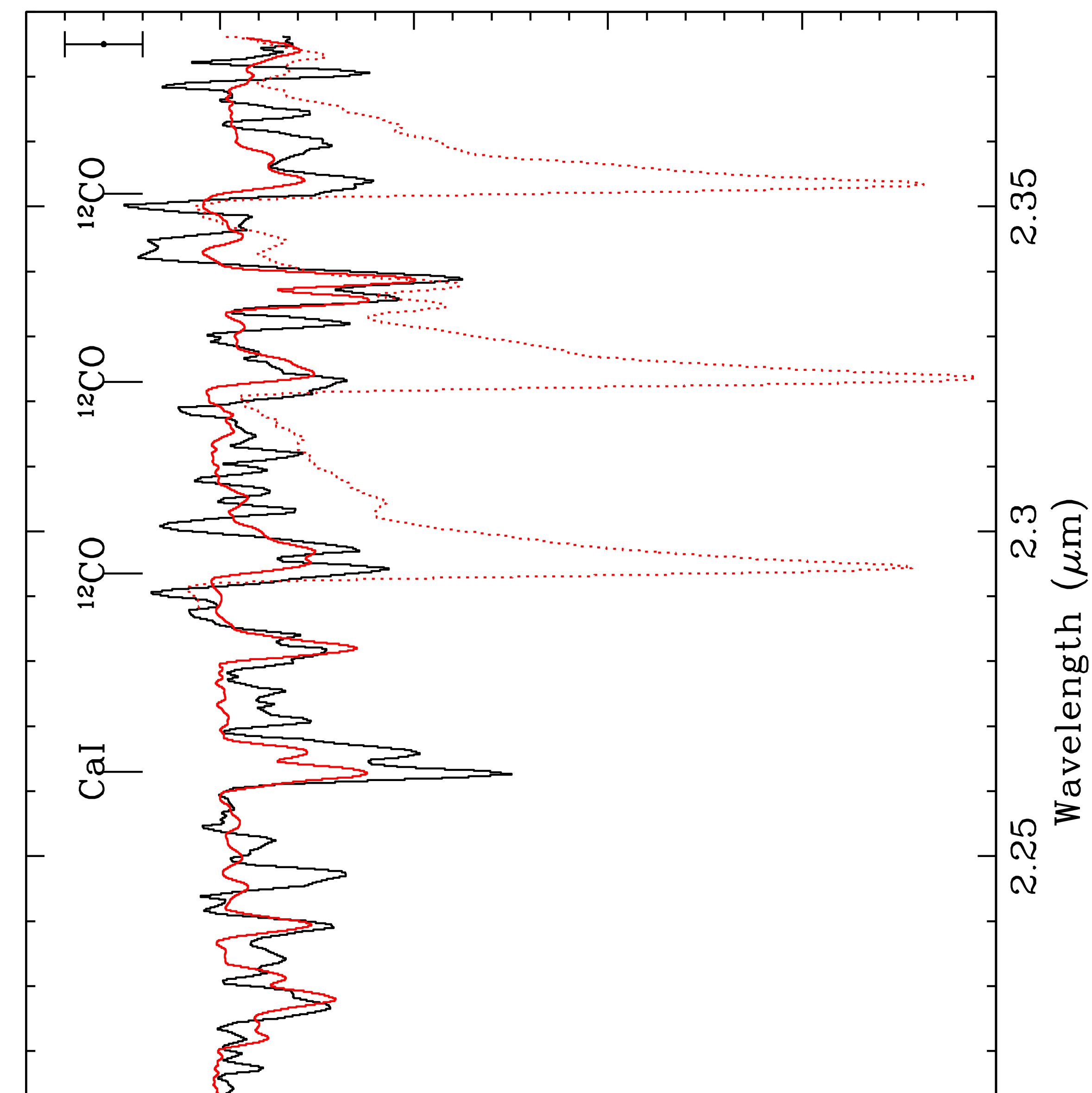

f8.eps

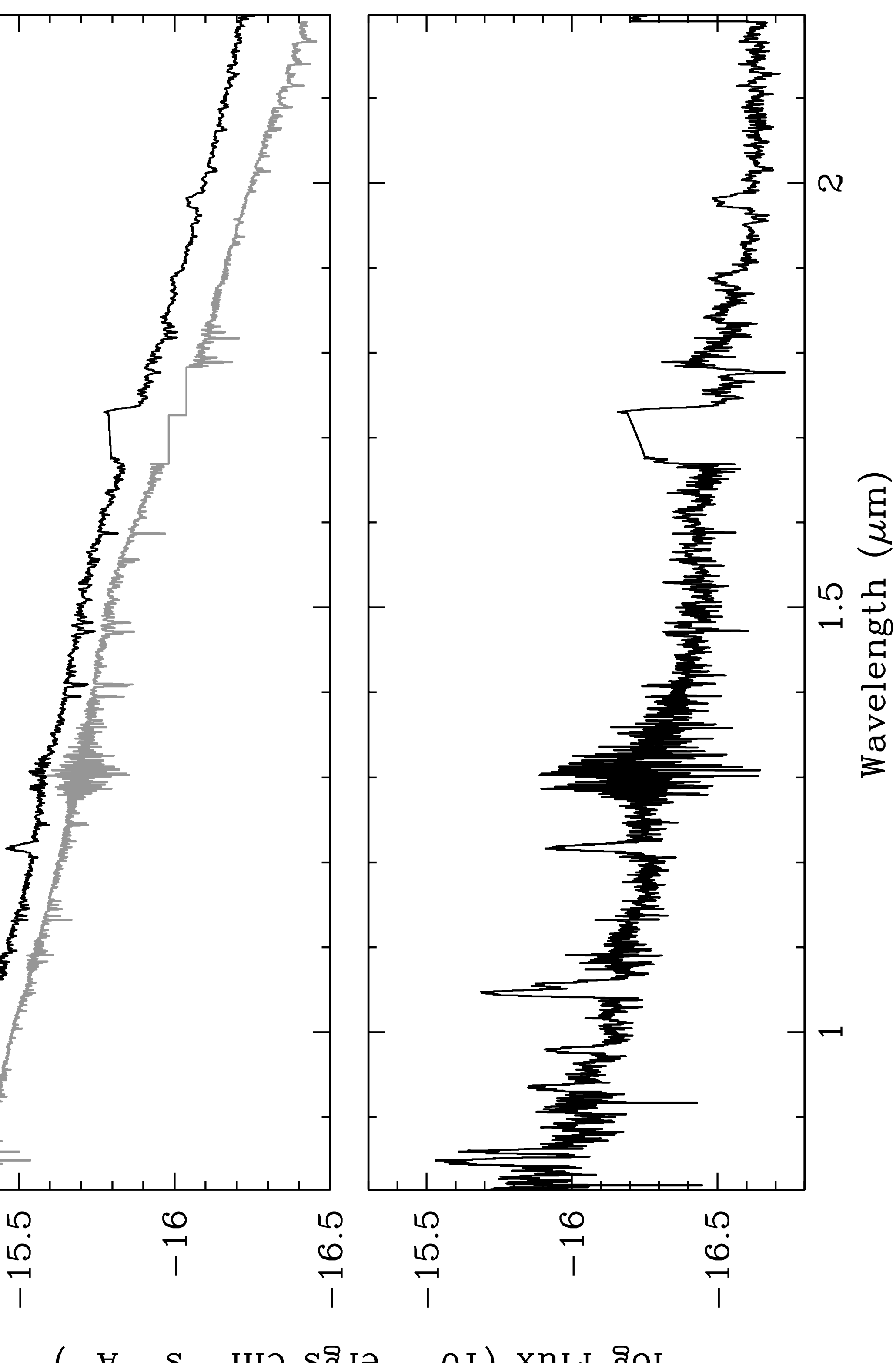

f9.eps